AGU ADVANCING EARTH AND SPACE SCIENCE

Geophysical Research Letters

RESEARCH LETTER
10.1029/2020GL087019

Bathymetry-Constrained Navigation of Argo Floats Under Sea Ice on the Antarctic Continental Shelf

L. O. Wallace[1], E. M. van Wijk[2,3], S. R. Rintoul[2,3,4], and B. Hally[1]

[1]School of Science, RMIT University, Melbourne, Victoria, Australia, [2]CSIRO Oceans and Atmosphere, Hobart, Tasmania, Australia, [3]Australian Antarctic Program Partnership, University of Tasmania, Hobart, Tasmania, Australia, [4]Centre for Southern Hemisphere Oceans Research, Hobart, Tasmania, Australia

Key Points:
- Sea ice prevents profiling floats from surfacing and obtaining a position from navigation satellites, reducing the utility of observations
- Floats programmed to park on the seabed between profiles provide year-round, full-depth profiles in an Antarctic continental shelf polynya
- Float measurements of pressure at the seabed were used in combination with known bathymetry to estimate the location of under-ice profiles

Supporting Information:
- Supporting Information S1

Correspondence to:
L. O. Wallace,
luke.wallace2@rmit.edu.au

Citation:
Wallace, L. O., van Wijk, E. M., Rintoul, S. R., & Hally, B. (2020). Bathymetry-constrained navigation of Argo floats under sea ice on the Antarctic continental shelf. *Geophysical Research Letters*, *47*, e2020GL087019. https://doi.org/10.1029/2020GL087019

Received 8 JAN 2020
Accepted 7 MAY 2020
Accepted article online 12 MAY 2020

Abstract Antarctic continental shelf waters are poorly sampled, particularly beneath sea ice during winter. Profiling floats could help fill this gap, but floats are unable to surface to obtain a satellite position when ice is present. We deployed Argo profiling floats in a coastal polynya with a novel mission to rest on the sea floor between profiles. "Parking" on the seabed minimized the drift of the floats and allowed year-round, full-depth measurements over multiple winters. Measurements of water depth derived from the floats were used in combination with known bathymetry to constrain the position of profiles collected under ice. Errors were quantified by withholding known positions and comparing them to estimated positions; the bathymetrically constrained algorithm outperformed linear interpolation. A similar approach could potentially be used to geolocate other under-ice oceanographic platforms that measure water depth.

Plain Language Summary The seasonal ice zone of the Antarctic continental shelf is one of the largest "blind spots" in the global oceans. Profiling float measurements can help fill this gap; however, sea ice prevents the floats from surfacing and obtaining a position from satellites. This reduces the utility of these data to the oceanographic community. We deployed floats in a novel way to rest on the seabed between profiles. "Parking" on the seabed helped retain the floats on the continental shelf and also provided measurements of sea floor depth as well as water properties. We used the water depths measured by the floats and knowledge of seabed bathymetry to estimate the position of the float profiles. The new approach offers significant improvement over the usual approach of linear interpolation and could potentially be used to navigate other oceanographic instruments under ice.

1. Introduction

Historically, few oceanographic observations have been made on the Antarctic continental shelf, especially in winter when sea ice restricts ship operations. This lack of observations has slowed progress in understanding critical climate phenomena, including ocean-driven melt of ice shelves, formation of Antarctic Bottom Water, and sea ice formation and melt.

Autonomous oceanographic platforms such as floats and gliders can help fill this observational gap. However, geolocation of mobile oceanographic instruments deployed under sea ice remains a challenge. A variety of navigation techniques (e.g., terrain-based, optical, inertial, and acoustic) have been developed for guiding platforms such as gliders and Autonomous Underwater Vehicles on missions under sea ice (Kimball & Rock, 2011; Lund-Hansen et al., 2018; McEwen et al., 2005; Melo & Matos, 2017; Webster et al., 2015). These techniques cannot typically be applied to passively drifting instruments like profiling floats, which have limited battery and payload capacity.

Argo is a global array of free-drifting floats that measure pressure, temperature, and salinity of the ocean. Profiling floats are typically geolocated with a Global Positioning System (GPS) satellite fix obtained at the sea surface. When ice is present, floats cannot reach the surface and communicate with the satellite. While the profile data collected under ice can be stored, the lack of position information limits the value of the profile. Missing positions are typically estimated using linear interpolation (e.g., Wong & Riser, 2011), but this can lead to large uncertainties in position, especially for extended periods under ice (Chamberlain et al., 2018). Additional information (e.g., conservation of potential vorticity) can help constrain float positions; however, mapping errors are large in regions of complex bathymetry (Reeve

et al., 2016). Floats can be tracked acoustically, as has been done in the Weddell Gyre (Klatt et al., 2007). However, this requires an array of moored sound sources, at substantially higher cost, and is not yet practical on a circumpolar scale. Therefore, new approaches for estimating the location of under-ice profiles are urgently needed by the oceanographic community.

Argo floats are typically deployed in water deeper than 2,000 m, to avoid contact with the seabed. Here, we assess the feasibility of using profiling floats to obtain oceanographic measurements on the Antarctic continental shelf. Floats were programmed in a novel way, to ground (or "park") on the seabed between profiles to keep them on the shelf for as long as possible. Here we describe a new algorithm that exploits the float measurement of pressure at the seabed (converted to water depth) together with known bathymetry to estimate the position of under-ice profiles. Errors in position are significantly reduced compared to the typical approach of linear interpolation.

2. Data and Methods

2.1. Profiling Floats

Argo floats were deployed in the Mertz polynya on the continental shelf near Adélie Land, East Antarctica, in 2012/2013 and 2015/2016. Floats profiled to the seabed every 5 days and were grounded on the bottom between profiles to reduce drift and aid retention on the shelf. To achieve this, the float "park pressure" was set to be deeper than the maximum depth expected on the continental shelf.

In 2012/2013, three Sounding Oceanographic Lagrangian Observer (SOLO) polar profiling floats (from Woods Hole Oceanographic Institution) collected data from the seabed to the surface when in open water, or to the underside of icebergs or sea ice while beneath ice. This float model has a ruggedized antenna that withstands contact with ice, unlike most ice-floats that are programmed to avoid ice. After each profile, the float makes repeated attempts to surface, in an attempt to find a lead in the ice through which to surface and telemeter data. If the float is unable to surface and stops ascending due to contact with ice, the shallowest pressure is a measure of the ice draft.

In 2015/2016, five Teledyne Webb Research APEX floats were deployed in the Mertz polynya. These floats utilize an ice sensing algorithm (Klatt et al., 2007) to avoid surface ice by using a measured temperature threshold (−1.81°C) in the surface layer as a proxy for the presence of ice above. If temperatures less than the threshold are encountered during ascent, the float aborts the ascent and descends to the seabed before performing the next profile. In this way, floats avoid contact with sea ice. Profiles collected by both float types while under ice are stored and transmitted when the float is next able to surface.

2.2. Float Path Prediction Algorithm

As the floats rest on the seabed between profiles, each profile includes a measurement of pressure at the sea floor, which can be converted to water depth (Saunders, 1981). We use this depth information to constrain estimates of the unknown location of each profile under ice. The algorithm seeks the shortest path between two known profile locations such that bottom depths measured by the float are consistent with the known bathymetry. We compare the bottom depths measured by the floats to the digital elevation model from Beaman et al. (2010), spanning 138–148°E, 63–69°S, with 0.005 arcdegree (~500 m) horizontal resolution.

The algorithm is illustrated in Figure 1. Starting from Profile 1 (with known position), the locus of possible positions for Profile 2 is defined by those locations with bottom depth close to the depth measured by the float and within a search radius defined by the speed of the float multiplied by the time between the two profiles. The intersection between the area of suitable depths and the area defined by the search radius defines the locus of possible positions for Profile 2. The locus of possible positions for the subsequent profile (Profile 3) is found in a similar way, searching from the edge of the polygon defining feasible positions of Profile 2. This procedure is carried out by simultaneously working forward from the last profile with known position and backward from the location of the first surfacing after a period beneath ice. The constraint that the two paths must meet in the middle eliminates many possible float paths.

In order to find the shortest feasible path, the algorithm is run iteratively. The drift speed is decreased with each iteration until either the polygons reach a user-defined minimum size known as the lockdown size (taken as known in subsequent iterations) or the user-defined minimum drift speed has been reached (see

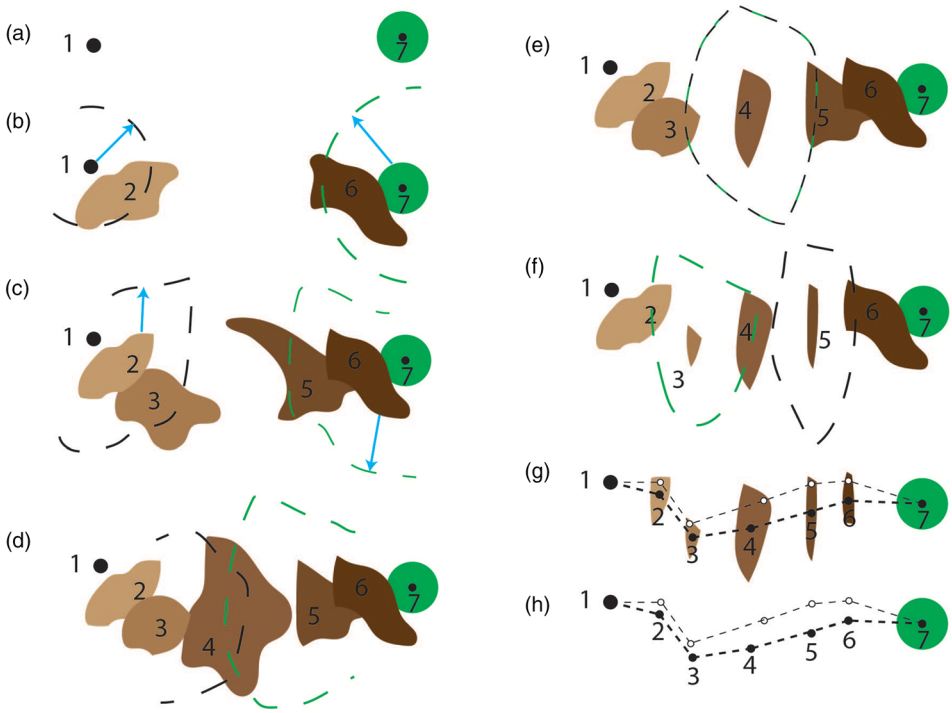

FIGURE 1. Algorithm schematic. (a) Two known positions (1 and 7) with five unknown positions in between. (b) Polygons indicate where float depth matches bathymetry. Polygons are further restricted by a search radius (dashed lines) set by the distance a float could travel between profiles at an assumed speed. (c) Search radius from the edge of polygons defined for Profiles 2 and 6 restricts polygons for 3 and 5. (d) Search radius from 3 and 5 restricts the polygon for 4. At this central profile, forward and backward searches meet, and only the intersection of the two polygons remains. (e) Search radius from 4 (in both directions) further refines polygons for 3 and 5. (f) Search radius from 3 and 5 refines polygons for 2 and 6. (g) The most likely profile location is either the centroid (solid circles) or the closest-matching depth (open circles). (h) Derived path for both options.

section 3.1.2). The default lockdown size is set to the area of a circle with a radius of 1.5 km, approximately equal to the accuracy of an Iridium position estimate (Meldrum, 2007); that is, the algorithm does not attempt to further reduce the size of the polygons once they are equivalent to the uncertainty in an Iridium satellite position fix. Note that the algorithm does not impose a minimum speed. If the polygons defining the feasible positions of two profiles are distant from each other, hence requiring rapid drift between them, the algorithm will not reduce this speed in later iterations.

The code allows for the final profile location to be selected as either the closest-matching depth or the centroid within each polygon (Figure 1h). In practice, the closest-matching depth can be multi-valued; therefore, in this study we have used the centroid for all analyses. Occasionally, the final polygon can consist of two or more discrete polygons with similar depths. In this case the algorithm selects the polygon with the maximum area as the most likely location. If more than one feasible trajectory is found, knowledge of the circulation from observations, models, or theory can be used to identify the most likely path.

3. Results

Floats deployed in the Mertz polynya in 2012 ($n = 2$) and 2015 ($n = 5$) were used to test the algorithm (Table 1). Float lifetimes ranged from 1.4 to 49 months. Four floats with the longest lifetimes (12 months to 4 years) spent periods from 3 to 13 months under ice without surfacing.

3.1. Algorithm Parameters

3.1.1. Depth Tolerance

The assumption that the maximum pressure measured by the float (converted to depth) is equal to the actual depth at the profile location (within a user-defined tolerance, $\pm \delta_{bath}$) was tested by comparing maximum float depth to known bathymetry at profiles with a known position (Figure 2a). The two measurements are highly correlated ($r^2 = 0.96$). The root mean square difference between the two measurements is

Table 1
Float Longevity and Position Information

Float number (wmoid)	Date of first profile	Date of last profile	No. of profiles (float longevity in months)	No. of profiles with GPS position	No. of profiles with Iridium position	No. of under-ice profiles without a position	Longest period under ice: No. of profiles (duration in days)
7900330	16/01/12	31/03/12	16 (2.5)	5	1	10	7 (40)
7900331	11/01/12	31/03/14	163 (27)	5	10	148	74 (375)
7900604	15/01/15	17/02/16	80 (13)	18	0	62	45 (230)
7900605	15/01/15	14/07/15	37 (12)	8	0	29	18 (95)
7900606	15/01/15	01/03/15	10 (1.5)	7	0	3	2 (15)
7900607	16/01/15	19/02/15	8 (1.4)	6	0	2	2 (15)
7900608[a]	18/01/15	01/03/19[a]	205 (49)	29	0	74	51 (260)

[a]7900608 left the continental shelf at 21/03/2016.

51 m, or 24 m when restricted to regions with bathymetric slope less than 8% (Figure 2b). We used a value of 30 m for the depth tolerance (δ_{bath}), equal to one standard deviation of the difference between maximum profile depth and bathymetry for profiles with known positions and bottom slope <8%. As expected, differences between float depth and actual depth are larger in regions with steep or rapidly changing topography. The depth tolerance was therefore defined as a function of bottom slope (Figure 2b). For slopes between 8% and 12%, the depth tolerance was calculated as $\delta_{bath} \times (1 + (\text{slope} - 8)/4)$ and for slopes greater than 12%, as $\delta_{bath} \times 2$.

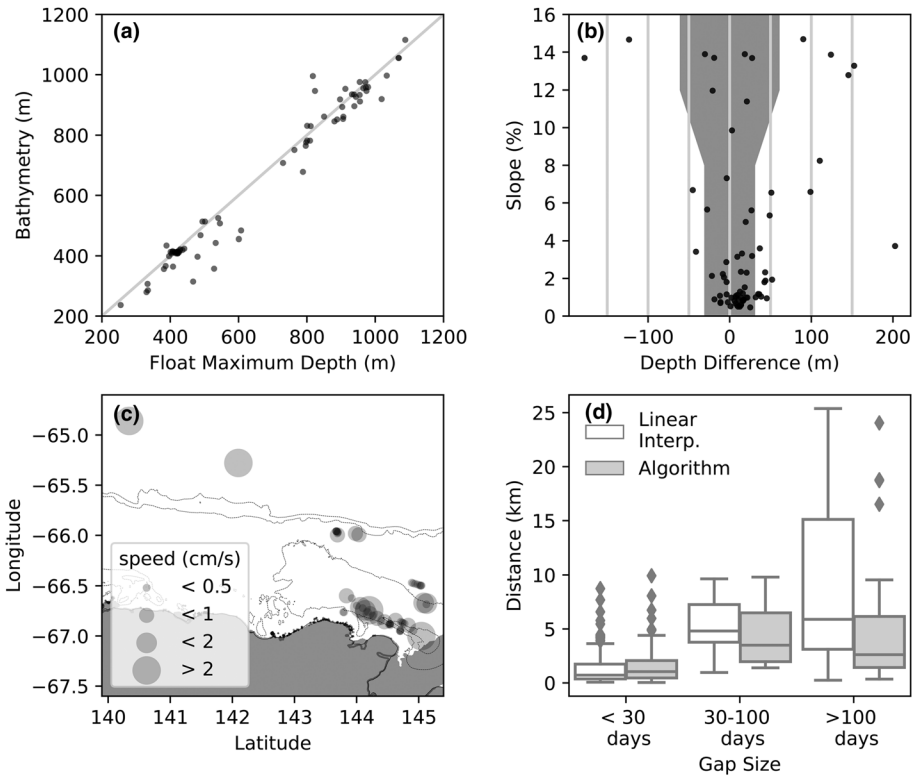

FIGURE 2. (a) Bathymetry versus maximum float depth at known locations. (b) Difference between bathymetry and float maximum depth at known locations against bathymetric slope. Shaded region represents the slope-dependent depth tolerance ($\pm \delta_{bath}$). (c) Float speed between profiles with known locations, for all floats, bathymetry from Beaman et al. (2010). (d) Box plot of the median error in position for different length gaps between known profiles, where the error is the difference in distance between predicted and known positions of withheld profiles. Sample size for each time period: <30 days ($n = 116$), 30–100 days ($n = 19$), and >100 days ($n = 37$). Diamonds are outliers (>1.5 times the interquartile range [IQR] between the 25th and 75th percentiles) from the upper and lower quartiles.

3.1.2. Float Drift Speed

The algorithm iterates from user-defined maximum to minimum speeds to define the search radius at each iteration. The distance traveled between known locations provides an indication of likely speeds. Figure 2c shows the drift speeds between known locations with no more than two unknown locations between them. Drift speeds between profile locations on the continental shelf were low, as expected for floats that are parked on the seabed between profiles. The mean speed for all floats was 0.9 ± 1.3 cm s^{-1}. Float speeds on the shelf exceeded 2 cm s^{-1} on only four occasions, with a maximum speed of 6.6 cm s^{-1}. By starting with the largest reasonable drift speed and then reducing the speed with each iteration, the algorithm progressively reduces the area of feasible locations and finds the shortest path consistent with the observed bathymetry. In this case, we iteratively reduced the speed from a maximum of 10 cm s^{-1} to a minimum speed of 0.01 cm s^{-1}, in steps of 0.01 cm s^{-1}. Supporting information Figure S1 shows that the histogram of algorithm-derived speeds is similar to the histogram of speeds between known profiles, with a median speed of 0.3 cm s^{-1} in both cases.

3.2. Algorithm Validation

One approach to quantify the skill of the algorithm is to predict the location of withheld (known) positions ($n = 89$, from seven floats, Table 1). We created 171 artificial gaps of various sizes by withholding known positions; the difference between known and predicted positions was taken as a measure of the error (Figure 2d; see also Figure S2). The algorithm and linear interpolation produced similar median errors for gaps between known positions of less than 30 days (1.0 km). As the floats are parked on the seabed between profiles, drift speeds are low and the floats do not move far; hence, the interpolation method makes little difference over short periods. The algorithm outperformed linear interpolation for gaps longer than 30 days and in regions of complex bathymetry. For gaps between known profiles longer than 100 days, the algorithm estimated positions with a median error of 2.6 km (with 75% estimated to within 6 km), compared to linear interpolation with a median error of 5.9 km and 75% estimated to within 15 km. The depth-constrained approach resulted in position errors larger than 10 km in only four cases, all in areas of flat topography where bathymetry provided little constraint on the float path.

However, several caveats apply to this assessment of the errors. To date, few floats have been deployed on the Antarctic continental shelf, and we are restricted to a small data set, particularly for longer periods under ice. Moreover, the temporal sampling of the shelf floats results in an uneven distribution of known locations through the year. These floats typically return a tight cluster of known positions during summer, followed by long gaps under ice in winter (with only a few known positions), and another tight cluster of known positions during the following summer. Very long gaps coincide with the winter period, and the floats only sample a few winters. Note that the gap sizes in Figure 2d refer to the separation in time between profiles with known positions. For long under-ice periods (>100 days) the gap in time between the withheld position and the nearest known position may be considerably less than 10 profiles (50 days) away from a known position. Given the slow drift of these floats, this gap generally corresponds to a shorter distance over the ground, skewing the results toward lower errors for both methods. Errors are likely larger over longer under-ice periods, but we have only a few examples and therefore cannot derive reliable statistics from this small sample. A similar validation exercise using the subset of known positions should be carried out once a larger data set of shelf float profiles becomes available or when using the algorithm in a new application or region.

An alternative approach to assess the performance of the methods over long gaps is to make a direct comparison of the paths obtained using the algorithm and linear interpolation and their compatibility with other information (Figure 3). SOLO float 7900331 survived 2 years on the shelf including two long periods under ice: March to November 2012 (275 days) and December 2012 to December 2013 (375 days). The first under-ice gap between Profiles 9 and 64 is depicted in Figure 3a. Bottom depths along the linearly interpolated path (red) differ from the maximum depths recorded by the float (black) by as much as 150 m (Figure 3b). The depth-constrained path (yellow) agrees with the bottom depths measured by the float, as expected. The derived float trajectory is also consistent with float drift between known positions and with the cyclonic circulation in the Adélie Depression inferred from oceanographic surveys (Lacarra et al., 2011; Martin et al., 2017; Williams et al., 2010) and numerical simulations (Cougnon et al., 2017; Kusahara et al., 2017).

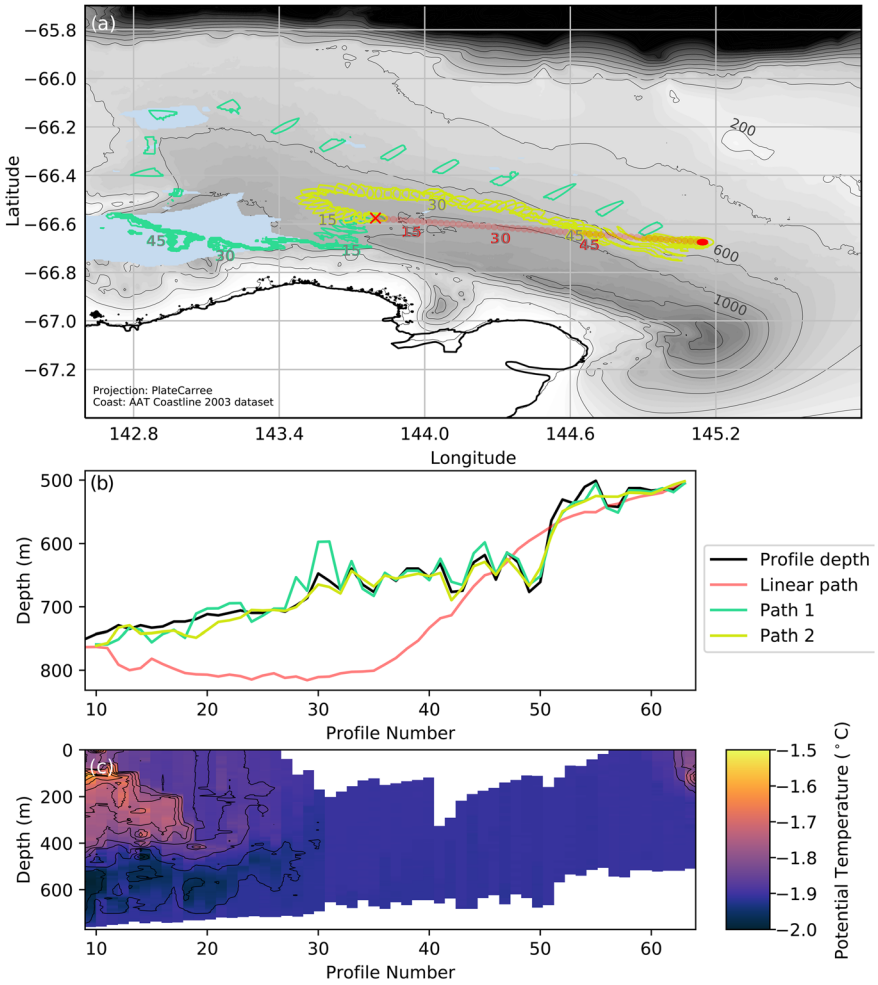

FIGURE 3. (a) Algorithm-derived paths for the under-ice period for float 7900331 between Profiles 9 (red cross) and 64 (red circle), selected profiles labeled: red = linear interpolation; yellow = depth constraint; green = iceberg and depth constraints. Iceberg mask (blue shading) digitized from satellite imagery. (b) Depth from Beaman et al. (2010) bathymetry at the location of each profile for each float path; black = depth measured by the float. (c) Potential temperature measured by the float. The float was under an iceberg(s) between Profiles 26 and 54.

The depth-constrained path however cannot account for a 4-month period during which the float recorded large minimum pressures, indicating the float had drifted under one or more large icebergs with drafts of 70 to 330 m (Figure 3c). The encounter with the iceberg(s) provides an additional constraint on the float path. An iceberg mask was defined using the position of large tabular icebergs (>1 km in size) identified in MODIS satellite imagery during the period of deployment (Figure 3a). The algorithm was then run requiring that the path be consistent with both the depth and iceberg constraints (specifically, profiles with a minimum pressure greater than a user-defined threshold [60 dbar] were required to fall within the iceberg mask [green path, Figure 3a]). The iceberg- and depth-constrained path, taken as our best estimate of the float trajectory, differed from both the linearly interpolated and depth-constrained paths by as much as ~100 km for particular profiles. For these long under-ice periods, the uncertainty in predicted location is significantly larger than the median error estimated by withholding known positions, particularly for profiles that are far from a known position (e.g., compare the difference in predicted locations for Profiles 15 and 30 in Figure 3a). Additional examples of depth-constrained and linearly interpolated trajectories are shown in the supporting information (Figures S3–S9).

4. Discussion and Conclusions

The continental shelf waters of Antarctica are poorly sampled, particularly in winter, when sea ice makes access difficult. Moored instruments can provide year-round measurements (e.g., Snow et al., 2018) but

require expensive ship visits and are generally limited to sampling below the depth of iceberg drafts (>300 m or more). Profiling floats can help fill this gap by providing year-round, full-depth measurements. We have shown that floats parked on the seabed between profiles can survive multiple encounters with the sea floor and remain on the shelf for several years. A similar "park-on-the-bottom" approach was used for profiling float deployments in the Ross Sea from 2013-2017 (Porter et al., 2019). However, floats cannot surface when under ice, and therefore, the position of the under-ice profiles is unknown. The lack of position information reduces the utility of these valuable under-ice observations.

Here we have presented a novel bathymetry-constrained approach to under-ice navigation of autonomous platforms. Floats that profile to the sea floor provide a measurement of pressure at the seabed (hence water depth) at each profile. In areas of known bathymetry, the measured depths can be used to constrain the trajectory of the float. The algorithm we developed to exploit this information finds the shortest path consistent with the measured bottom depths, working forward and backward from profiles with known positions.

This approach works well in regions where the bathymetry is well known and variable (in the limiting case of constant water depth, the measured depth provides no useful constraint). In the case of the Adélie Land shelf, where the bathymetry is characterized by a deep depression bounded by shallow banks, the algorithm produces well-defined trajectories, even for long periods (months to years) between known positions. Glacially scoured troughs like the Adélie Depression are common on the Antarctic continental shelf; hence, the method is potentially widely applicable. Less than 18% of the global ocean seabed has been mapped at a resolution of 1 km (Mayer et al., 2018). Despite this, many sectors of the Antarctic continental shelf have bathymetry resolved to 500 m or better (i.e., large sectors of the Ross, Amundsen and Bellingshausen Seas, western Antarctic Peninsula, and Adélie Land) (e.g., Wölfl et al., 2019) and are good candidates for this approach. On other parts of the continental shelf, bathymetry remains poorly known, and the algorithm is likely to be less useful until improved bathymetry data become available.

The method outperforms linear interpolation, providing paths that are consistent with observed depths along the trajectory and that have smaller errors when assessed by predicting withheld positions. In general, errors in the inferred trajectory, and the ability to quantitatively assess the errors, will depend on a number of factors, including the number and location of profiles with known positions, the duration of the under-ice period, the speed of the float, the nature of the bathymetry, and the availability of additional information with which to constrain or validate the float path. Comparison of the distribution of speeds between known positions to the distribution of speeds after optimization (e.g., Figure S1) provides a useful consistency check: A large discrepancy may suggest, for example, that the user-defined maximum/minimum speeds need to be adjusted.

The algorithm seeks the shortest path consistent with the water depth measured by the float. If additional information is available (e.g., knowledge that the float was under an iceberg for part of its drift or that the velocity in a particular region is known [e.g., clockwise flow in a gyre]), the inferred trajectory will likely be longer than the shortest path found without this constraint. In our case, the depth- and iceberg-constrained path differed from the depth-constrained and linearly interpolated paths by ~100 km. Chamberlain et al. (2018) noted errors of similar magnitude comparing linearly interpolated positions to trajectories of acoustically tracked floats that spent 8 months beneath ice in the Weddell Sea. Wong and Riser (2011) found that linearly interpolated positions underestimated the distance between under-ice profiles by an average of 20 km for consecutive profile pairs (10 days apart) compared to ice-free periods. This could be considered a lower bound on position uncertainty for drifting floats (which drift more quickly than the grounded floats considered here), given that under-ice periods are often many months or longer. We note that the floats considered here tend to roughly follow depth contours, but not strictly so (see Figure 3b, where float depth reduces from 700 to 500 m over 6 cycles [30 days]). Interpolation methods that assume that floats follow depth contours (or contours of constant planetary vorticity, f/H, where f is the Coriolis parameter and H is the water depth) will likely be less accurate than methods that require float measurements of bottom depth to match known bathymetry.

While our method cannot be used to navigate under-ice profiles collected by free-drifting Argo floats that do not reach the seabed, the technique can be used to derive under-ice positions of deep Argo floats that measure to the seabed. Between 2000 and 2018, 18% of the 55,000 (~10,000) Argo profiles collected south of 60°S were under-ice. We expect similar statistics to apply to the deep Argo array as it expands. However, as deep

floats may drift hundreds of meters above the seabed during their park phase, they are likely to travel larger distances between profiles. Moreover, deep floats may transit regions of the global oceans where the bathymetry is flat or poorly known. Further work will be required to characterize the errors and fine-tune the approach as the number of deep Argo floats deployed in the sea ice zone increases.

A similar approach could potentially be applied to other platforms operating under ice, where the position of the platform is unknown or uncertain. For example, gliders and underwater vehicles often use acoustics to measure water depth with recent advances including the integration of multibeam echosounders and scanning sonars for seabed and iceberg mapping (Wölfl et al., 2019; Zhou et al., 2019). Our simple depth-based approach could provide an additional constraint on geolocation in areas of known bathymetry. Seals tagged with oceanographic sensors can provide a bottom depth measurement when foraging on the seabed. Padman et al. (2010), for example, used seal profiles to improve bathymetric maps of the continental shelf of the western Antarctic peninsula. Characteristics of the dive behavior show that approximately 30% of Elephant and Weddell seal dives are benthic foraging dives (Nachtsheim et al., 2019; Padman et al., 2010), with most dives on the continental shelf reaching the seabed (McConnell & Fedak, 1996). The Argos satellite positions obtained by the seals are less accurate than GPS and may be in error by tens to hundreds of kilometers (e.g. Table 1, Costa et al., 2010). The algorithm presented here could be adapted to reduce the uncertainty in the location of benthic seal profiles over the continental shelf.

The ice-covered ocean at high southern latitudes is one of the largest "blind spots" in the global ocean observing system, with measurements particularly scarce on the continental shelf (Rintoul et al., 2014). Our results show that conventional profiling floats can help fill this gap. First, floats parked on the seabed between profiles survive repeated encounters with the sea floor and remain on the continental shelf for multiple years, providing unprecedented year-round profiles of the entire water column. Second, the profiles can be geolocated over long periods without a satellite position fix using a depth-constrained optimization algorithm. These two advances demonstrate that sustained, year-round, full-depth observations of ocean properties on the Antarctic continental shelf are now possible.

Acknowledgments
We thank two anonymous reviewers for their constructive and insightful comments that helped to improve this manuscript. This research was supported by the Australian Antarctic Program Partnership; CSIRO; the Earth Systems and Climate Change Hub of the Australian Government's National Environmental Science Program; the Australian Antarctic Science Program; the Antarctic Gateway Partnership; Australia's Integrated Marine Observing System; and the Centre for Southern Hemisphere Oceans Research. Algorithm and float data are available online (from https://gitlab.com/sfmninja/pyfluid and https://doi.org/10.6084/m9.figshare.12015126).

References

Beaman, R. J., O'Brien, P. E., Post, A. L., & De Santis, L. (2010). A new high-resolution batyhmetry model for the Terre Adélie and George V continental margin, East Antarctica. *Antarctic Science*, *23*(1), 95–103. https://doi.org/10.1017/S095410201000074X

Chamberlain, P. M., Talley, L. D., Mazloff, M. R., Riser, S. C., Speer, K., Gray, A. R., & Schwartzman, A. (2018). Observing the ice-covered Weddell Gyre with profiling floats: Position uncertainties and correlation statistics. *Journal of Geophysical Research: Oceans*, *123*, 8383–8410. https://doi.org/10.1029/2017JC012990

Costa, D. P., Robinson, P. W., Arnould, J. P. Y., Harrison, A.-L., Simmons, S. E., Hassrick, J. L., et al. (2010). Accuracy of ARGOS Locations of Pinnipeds at-Sea Estimated Using Fastloc GPS. *PLoS ONE*, *5*(1), e8677. https://doi.org/10.1371/journal.pone.0008677

Cougnon, E. A., Galton-Fenzi, B. K., Rintoul, S. R., Legrésy, B., Williams, G. D., Fraser, A. D., & Hunter, J. R. (2017). Regional changes in icescape impact shelf circulation and basal melting. *Geophysical Research Letters*, *44*, 11,519–11,527. https://doi.org/10.1002/2017GL074943

Kimball, P., & Rock, S. (2011). Sonar-based iceberg-relative navigation for autonomous underwater vehicles. *Deep Sea Research, Part II*, *58*, 1301–1310. https://doi.org/10.1016/j.dsr2.2010.11.005

Klatt, O., Boebel, O., & Fahrbach, E. (2007). A profiling float's sense of ice. *Journal of Atmospheric and Oceanic Technology*, *24*, 1301–1308. https://doi.org/10.1175/JTECH2026.1

Kusahara, K., Hasumi, H., Fraser, A. D., Aoki, S., Shimada, K., Williams, G. D., et al. (2017). Modelling ocean-cryosphere interactions off Adélie and George V Land, East Antarctica. *Journal of Climate*, *30*(1), 163–188. https://doi.org/10.1175/JCLI-D-15-0808.1

Lacarra, M., Houssais, M.-N., Sultan, E., Rintoul, S. R., & Herbaut, C. (2011). Summer hydrography on the shelf off Terre Adélie/George V Land based on the ALBION and CEAMARC observations during the IPY. *Polar Science*, *5*(2), 88–103. https://doi.org/10.1016/j.polar.2011.04.008

Lund-Hansen, L. C., Juul, T., Eskildsen, T. D., Hawes, I., Sorrell, B., Melvad, C., & Hancke, K. (2018). A low-cost remotely operated vehicle (ROV) with an optical positioning system for under-ice measurements and sampling. *Cold Regions Science and Technology*, *151*, 148–155. https://doi.org/10.1016/j.coldregions.2018.03.017

Martin, A., Houssais, M.-N., le Goff, H., Marec, C., & Dausse, D. (2017). Circulation and water mass transports on the East Antarctic shelf in the Mertz Glacier region. *Deep Sea Research, Part I*, *126*, 1–20. https://doi.org/10.1016/j.dsr.2017.05.007

Mayer, L., Jakobsson, M., Allen, G., Dorschel, B., Falconer, R., Ferrini, V., et al. (2018). The Nippon Foundation—GEBCO Seabed 2030 Project: The Quest to See the World's Oceans Completely Mapped by 2030. *Geosciences*, *8*(2), 63. https://doi.org/10.3390/geosciences8020063

McConnell, B. J., & Fedak, M. A. (1996). Movement of southern elephant seals. *Canadian Journal of Zoology*, *74*(8), 1485–1496. https://doi.org/10.1139/z96-163

McEwen, R., Thomas, H., Weber, D., & Psota, F. (2005). Performance of an AUV navigation system at Arctic latitudes. *IEEE Journal of Oceanic Engineering*, *139*(2), 250–264. https://doi.org/10.1016/j.oceaneng.2017.04.047

Meldrum, D. (2007). Iridium location quality: Is it good enough for drifters? Proc. Data Buoy Cooperative Panel Scientific and Technical Workshop, Jeju, South Korea, WMO-IOC, 6. https://www.wmo.int/pages/prog/amp/mmop/documents/dbcp/Dbcp32/presentations/06_Meldrum_Iridium_Loc_QC.pdf

Melo, J., & Matos, A. (2017). Survey on advances on terrain based navigation for autonomous underwater vehicles. *Ocean Engineering*, *139*, 250–264. https://doi.org/10.1016/j.oceaneng.2017.04.047

Nachtsheim, D. A., Ryan, S., Schröder, M., Jensen, L., Oosthuizen, W. C., Bester, M. N., et al. (2019). Foraging behaviour of Weddell seals (Leptonychotes weddellii) in connection to oceanographic conditions in the southern Weddell Sea. *Progress in Oceanography*, *173*(2019), 165–179. https://doi.org/10.1016/j.pocean.2019.02.013

Padman, L., Costa, D. P., Bolmer, S. T., Goebel, M. E., Huckstadt, L. A., Jenkins, A., et al. (2010). Seals map bathymetry of the Antarctic continental shelf. *Geophysical Research Letters*, *37*, L21601. https://doi.org/10.1029/2010GL044921

Porter, D. F., Springer, S. R., Padman, L., Fricker, H. A., Tinto, K. J., Riser, S. C., et al. (2019). Evolution of the Seasonal Surface Mixed Layer of the Ross Sea, Antarctica, Observed With Autonomous Profiling Floats. *Journal of Geophysical Research: Oceans*, *124*, 4934–4953. https://doi.org/10.1029/2018JC014683

Reeve, K. A., Boebel, O., Kanzow, T., Strass, V., Rohardt, G., & Fahrbach, E. (2016). A gridded data set of upper-ocean hydrographic properties in the Weddell Gyre obtained by objective mapping of Argo float measurements. *Earth System Science Data*, *8*(1), 15–40. https://doi.org/10.5194/essd-8-15-2016

Rintoul, S., van Wijk, E., Wåhlin, A., Taylor, F., Newman, L., Ackley, S., et al. (2014). *Seeing below the ice: A strategy for observing the ocean beneath Antarctic sea ice and ice shelves*. Hobart, Australia: *SOOS Report*. http://soos.aq/images/soos/activities/cwg/oasiis/SOOS-UnderIceStrategy.pdf.

Saunders, P. M. (1981). Practical conversion of pressure to depth. *Journal of Physical Oceanography*, *11*(4), 573–574. https://doi.org/10.1175/1520-0485(1981)011<0573:PCOPTD>2.0.CO;2

Snow, K., Rintoul, S. R., Sloyan, B. M., & Hogg, A. M. (2018). Change in Dense Shelf Water and Adélie Land Bottom Water precipitated by iceberg calving. *Geophysical Research Letters*, *45*, 2380–2387. https://doi.org/10.1002/2017GL076195

Webster, S. E., Freitag, L. E., Lee, C. M. & Gobat, J. I. (2015). Towards real-time under-ice acoustic navigation at mesoscale ranges. Paper presented at 2015 IEEE International Conference on Robotics and Automation (ICRA), Seattle, Washington, USA.

Williams, G. D., Aoki, S., Jacobs, S. S., Rintoul, S. R., Tamura, T., & Bindoff, N. L. (2010). Antarctic Bottom Water from the Adélie and George V Land coast, East Antarctica (140–149°E). *Journal of Geophysical Research*, *115*, C04027. https://doi.org/10.1029/2009JC005812

Wölfl, A.-C., Snaith, H., Amirebrahimi, S., Devey, C. W., Dorschel, B., Ferrini, V., et al. (2019). Seafloor mapping—The challenge of a truly global ocean bathymetry. *Frontiers in Marine Science*, *6*, 283. https://doi.org/10.3389/fmars.2019.00283

Wong, A. P. S., & Riser, S. C. (2011). Profiling float observations of the upper ocean under sea ice off Wilkes Land coast of Antarctica. *Journal of Physical Oceanography*, *41*(6), 1102–1115. https://doi.org/10.1175/2011JPO4516.1

Zhou, M., Bachmayer, R., & deYoung, B. (2019). Mapping the underside of an iceberg with a modified underwater glider. *Journal of Field Robotics*, *36*(6), 1102–1117. https://doi.org/10.1002/rob.21873